# Stable but Responsive Cloth

Kwang-Jin Choi          Hyeong-Seok Ko

Graphics and Media Lab
Seoul National University

## Abstract

We present a semi-implicit cloth simulation technique that is very
stable yet also responsive. The stability of the technique allows
the use of a large fixed time step when simulating all types of fab-
rics and character motions. The animations generated using this
technique are strikingly realistic. Wrinkles form and disappear in a
quite natural way, which is the feature that most distinguishes tex-
tile fabrics from other sheet materials. Significant improvements
in both the stability and realism were made possible by overcom-
ing the *post-buckling instability* as well as the numerical instabil-
ity. The instability caused by buckling arises from a structural in-
stability and therefore cannot be avoided by simply employing a
semi-implicit method. Addition of a damping force may help to
avoid instabilities; however, it can significantly degrade the realism
of the cloth motion. The method presented here uses a particle-
based physical model to handle the instability in the post-buckling
response without introducing any fictitious damping.

**Keywords:** Deformations, Numerical Analysis, Physically Based
Animation, Physically Based Modeling

**CR Categories:** I.3.7 [Computer Graphics]: Three-Dimensional
Graphics and Realism—Animation; G.1.7 [Numerical Analysis]:
Ordinary Differential Equations—Convergence and stability, Stiff
equations I.6.5 [Simulation and Modeling]: Model Development

## 1 Introduction

A normal outfit covers more than 90 percent of the human body.
Therefore, the realistic animation of cloth is imperative if we are to
animate humans to a satisfactory level of detail and realism. Over
the last decade a great deal of research has been dedicated to sim-
ulating cloth motion [Terzopoulos and Fleischer 1988; Carignan
et al. 1992; Breen et al. 1994; Courshesnes et al. 1995; Provot 1995;
Eberhardt et al. 1996; Eischen et al. 1996; Baraff and Witkin 1998;
Desbrun et al. 1999; Volino and Magnenat-Thalmann 2000]. All
of the methods proposed to date boil down to numerically solving
an ordinary differential equation, although they differ in regard to
characteristics such as stability, allowed time step size, etc.

Cloth is characterized by strong resistance to stretch and weak
resistance to bending, which leads to a stiff set of equations and
thus prohibits the use of large time steps. However, cloth simulation
techniques must be stable and fast if they are to be of practical use.

Previous studies have shown that implicit methods are well suited
to solving stiff equations with a reasonable step size, and successful
results have been reported in [Baraff and Witkin 1998; Volino and
Magnenat-Thalmann 2000].

Another property that is crucial to the appearance of fabrics in
motion is their buckling behavior. The buckling of fabrics is the
process by which wrinkles form, and leads to structures such as
those shown in Figure 1. The buckling of textile fabrics has a quite
different nature from solid materials [Amirbayat and Hearle 1989],
thus animation of a cloth would not look natural without having
such property. Nevertheless it has been largely ignored though
its problematic nature (instability and non-linearity) was recently
pointed out by [Eischen et al. 1996] and [Yu et al. 2000]. This pa-
per presents a stable and practical solution to this problem.



Figure 1: Buckling of Real Fabrics

The buckling of a thin material involves a very unstable state,
regardless of whether it is rigid (e.g. aluminum sheet) or flexible
(e.g. fabrics). When a compressive force is applied at the extremes
of a thin material, it initially resists changing shape. As this force is
increased, it eventually reaches the neutral equilibrium, the point at
which an infinitesimal increase or decrease in the force bifurcates
the situation in two radically different directions: increasing the
force leads to an unstable post-buckling response whereas the sys-
tem remains at stable equilibrium if the force is decreased. (Buck-
ling will be described in detail in Section 3.2.) Given that buck-
ling is a ubiquitous characteristic of fabrics, creating natural look-
ing cloth in an animation is very difficult without a stable way to
model this phenomenon.

The instability of the post-buckling response arises from a
structural instability [Bathe 1996], not from the stiff equations.
Therefore, the buckling instability cannot be overcome by simply
employing implicit methods. Some cloth simulation techniques
[Baraff and Witkin 1998; Volino and Magnenat-Thalmann 2000]
avoid this instability by adding damping forces[1]. The damping

---

[1]Damping is an important concept in this work. The Implicit method has
an intrinsic damping effect that comes from the formulation itself, which we
refer to as *artificial damping*. This damping is not related to the nature of
the cloth. On the other hand, we refer to damping that is deliberately added
to the formulation to simulate the nature of the cloth as *material intrinsic
damping*. A third kind of damping is sometimes added to enhance numerical
stability. We refer to this as *fictitious damping*. A damping term appearing

forces help to stabilize the physical system, or equivalently, they make the system matrix better conditioned and help to maintain positive definiteness in a semi-implicit formulation. However, the damping forces can significantly degrade the realism of the simulated cloth movement. For example, [Volino and Magnenat-Thalmann 2000] and [Volino and Magnenat-Thalmann 2001] found that the damping forces can lead to systems in which wrinkles will not form on the cloth surface, wrinkles resist disappearing, or even the fabrics resist falling under their own weight.

The artificial damping in implicit methods mainly affects the in-plane deformation of the cloth because the in-plane rigidity is much higher than the bending rigidity. Therefore, although artificial damping is expected to be partially responsible for the degradation of the quality of the out-of-plane movement of the cloth, we conjecture that the degradation in the quality mentioned above arises mainly from fictitious damping. The method we propose in this paper includes artificial damping (since it is an implicit method) and material intrinsic damping, but does *not* include fictitious damping. The need for fictitious damping is avoided through the use of the predicted static post-buckling response as an effective way to handle the instabilities associated with post-buckling situations. Because fictitious damping is not used, our method gives significantly more realistic cloth motion. This represents a significant step forward for the simulation of textile fabrics.

For solid materials, buckling signifies a failure and thus only the mechanics prior to buckling have been studied (e.g. determining the critical load on a column). Even in the study of textiles, there has been no significant result on the buckling process that can be applied to the dynamic simulation of cloth movement. Therefore, instead of physically simulating the unstable post-buckling dynamic response, we solve the instability problem by calculating the deformation energy of the shape at the predicted static equilibrium of the post-buckling state. We treat the numerical instability caused by stiff equations using implicit time stepping. Using the physical model outlined above and implicit time stepping, we could stably integrate the equation of motion with a large fixed time step and without the need for fictitious damping forces.

## 2 The Physical Model

Before we describe our particle-based physical model of fabrics, we discuss the problems in recently proposed physical models.

### 2.1 Problems in Previous Physical Models

Cloth is not a homogeneous continuum. Therefore modeling fabrics as a continuum and employing FEM or FDM has several potential drawbacks, a number of which are described in [Amirbayat and Hearle 1989]. One drawback of such methods is that they require a very fine meshing to produce large deformations. For a simulator to be practical in a computer graphics application, however, coarse discretization (about $1 \sim 5$ cm spacing between the nodal points) should be allowed to guarantee reasonable performance. In the analysis of almost incompressible and/or thin materials such as cloth, a continuum formulation with the elements at this scale might produce highly erratic results in the stress and strain [Bathe 1996], regardless of the interpolation order.

Another problem confronting the continuum approach is treating the divergence associated with buckling. [Eischen et al. 1996] used a non-linear shell model for cloth and performed finite element analysis to obtain the drape shape. They had to take special care and use measures such as arc length control to prevent divergence due to the non-linearity of the load-deflection curve or the



(a) all the connections for $P(i,j)$     (b) connections among neighboring particles in a particular direction
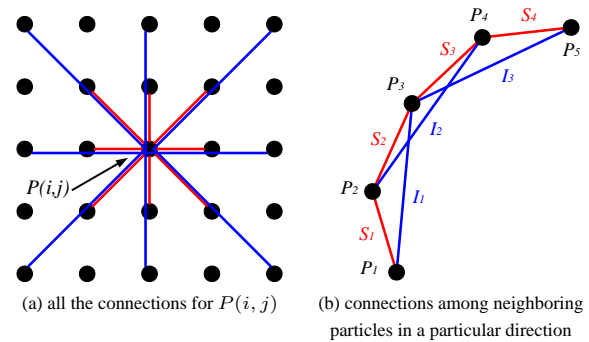
Figure 2: Connectivity of Interacting Particles

indefiniteness of the instantaneous stiffness matrix caused by buckling. [Yu et al. 2000] performed explicit dynamic simulation with fictitious viscous damping to avoid the divergence problem in the static analysis of the drape.

The fabric models in [Baraff and Witkin 1998] and [Courshesnes et al. 1995] are similar and can be understood as systems of connected flat triangles that are treated as a continuum. The in-plane deformation energy (or stress/strain relationship) of each triangle is derived from the continuum mechanics formulation. The bending deformation measure, on the other hand, is based on the angle between adjacent triangles. Therefore the fabric is not treated as a single homogeneous continuum and the bending and in-plane properties are modeled separately. The independent treatment of in-plane and out-of-plane cloth properties allows large bending deformation between triangles regardless of the in-plane rigidity of each triangle. However, the post-buckling instability can be a problem in this model, because each triangle is modeled as an almost incompressible material and the bending rigidity between triangles is very weak. Another problem of this physical model is that the bending characteristics largely depend on the triangulation. Since each triangle has very high in-plane rigidity, deformations tend to develop along the edges of the triangles. This causes a problem in systems comprised of aligned triangles because bending will occur along the edges. This problem can be cured by irregular triangulation, although this remedy introduces artificial flexural rigidity [Courshesnes et al. 1995]. As the triangulation becomes coarser, the artificial flexural rigidity will grow accordingly.

### 2.2 Using Interacting Particles

In our search for a way to overcome the drawbacks of the physical models outlined above, we found that systems of interacting particles are better suited for generating large deformations and handling the buckling problem. The method presented here draws on the idea that inspired the work of [Breen et al. 1994], who first applied the particle model to the simulation of textile fabrics. However, our particle model is much simpler than that used by Breen et al. and the treatment of compression and bending deformation is quite different from their approach. In this section, we describe the connectivity of the mass points representing the cloth surface. The associated energy functions and their derivatives are presented in the next section.

We approximate a cloth with a quadrilateral mesh of particles; thus each particle can be indexed as $P(i,j)$. Figure 2(a) shows all the connections associated with a given center particle. With the exception of particles at the boundaries, where some connections are broken, every particle has the connectivity shown in Figure 2(a). Two types of particle interaction model are employed, which are

---

in an equation may serve for both material intrinsic damping and fictitious damping.

referred to as *type 1* and *type 2*.

The *type 1* interaction model (red lines in Figure 2) is responsible for stretch and shear resistance. For this type of interaction, the particle $P(i, j)$ is connected to $P(i \pm 1, j)$, $P(i, j \pm 1)$, and $P(i \pm 1, j \pm 1)$. Such connections are referred to as sequential connections. The *type 2* interaction model (blue lines in Figure 2) is responsible for flexural and compression resistance. For type 2 interaction, the particles connected to $P(i, j)$ are $P(i \pm 2, j)$, $P(i, j \pm 2)$, and $P(i \pm 2, j \pm 2)$. Note that type 2 connections are made with every other particle, leading us to refer to them as *interlaced* connections. Figure 2(b) illustrates the sequential and interlaced connections in a particular direction, in which $S_1 \sim S_4$ are sequential connections and $I_1 \sim I_3$ are interlaced connections.

# 3 Energy Functions and Derivatives

In this section we first describe the *type 1* interaction model. We then elaborate on the concept of buckling and its profoundly different meanings in rigid materials and fabrics, after which we describe how this distinction is reflected in our handling of the post-buckling instability. Based on fabric-specific buckling behavior, we formulate the *type 2* interaction model. Finally, we add a material intrinsic damping to those models.

In the description of the energy functions and their derivatives presented below, the distinctive features of our formulation are highlighted by comparing the results of the proposed model with those presented in [Baraff and Witkin 1998] and [Volino and Magnenat-Thalmann 2000].

## 3.1 Type 1 Interaction

The $type1$ interaction is represented by a simple linear spring model, for which the energy function for particles $i$ and $j$ is,

$$E = \begin{cases} \frac{1}{2} k_s (|\mathbf{x}_{ij}| - L)^2 & : \quad |\mathbf{x}_{ij}| \geq L \\ 0 & : \quad |\mathbf{x}_{ij}| < L \end{cases} \quad (1)$$

where $\mathbf{x}_{ij} = \mathbf{x}_j - \mathbf{x}_i$, $L$ is the natural length, and $k_s$ is the spring constant. Note that this energy function accounts for the tension only. The force acting on particle $i$ due to the deformation between the two particles is,

$$\mathbf{f}_i = -\frac{\partial E}{\partial \mathbf{x}_i} = \begin{cases} k_s (|\mathbf{x}_{ij}| - L) \frac{\mathbf{x}_{ij}}{|\mathbf{x}_{ij}|} & : \quad |\mathbf{x}_{ij}| \geq L \\ 0 & : \quad |\mathbf{x}_{ij}| < L \end{cases} \quad (2)$$

The Jacobian matrix of the force vector is

$$\frac{\partial \mathbf{f}_i}{\partial \mathbf{x}_j} = \begin{cases} k_s \frac{\mathbf{x}_{ij} \mathbf{x}_{ij}^T}{\mathbf{x}_{ij}^T \mathbf{x}_{ij}} + k_s (1 - \frac{L}{|\mathbf{x}_{ij}|})(\mathbf{I} - \frac{\mathbf{x}_{ij} \mathbf{x}_{ij}^T}{\mathbf{x}_{ij}^T \mathbf{x}_{ij}}) & : \quad |\mathbf{x}_{ij}| \geq L \\ 0 & : \quad |\mathbf{x}_{ij}| < L \end{cases} \quad (3)$$

The first term tells us that the stiffness in the direction of the spring interaction is constant, which is an obvious consequence of modeling the interaction using a linear spring. The second term tells us that the stiffness orthogonal to the interaction direction is proportional to $(1 - \frac{L}{|\mathbf{x}_{ij}|})$. If we consider the 2-dimensional structure of the cloth, the direction orthogonal to all interactions corresponds to the out-of-plane direction. When the spring is stretched, in an implicit formulation, the second term plays an important role in stabilizing the spring because it introduces large positive eigenvalues of the system matrix in that direction. (If the same function were to be used for compression, the second term might turn the overall system matrix $(\mathbf{I} - \alpha \partial \mathbf{f}/\partial \mathbf{v} - \beta \partial \mathbf{f}/\partial \mathbf{x})$ indefinite since $k_s (1 - \frac{L}{|\mathbf{x}_{ij}|})$ is negative and can be arbitrarily large regardless of the time step size, as $|\mathbf{x}_{ij}| \to 0$. For this reason we do not use the same function

for compression. Compression is handled by the *type 2* interaction model, which is presented in Section 3.3.)

[Volino and Magnenat-Thalmann 2000] used the same spring model (i.e., $\frac{1}{2} k_s (|\mathbf{x}_{ij}| - L)^2$) for both stretching and compression in running a semi-implicit method. In their formulation, however, the second term of the Jacobian matrix in Equation 3 is omitted for both stretch and compression. They added a damping term to avoid null eigenvalues in the orthogonal direction. For a compressed spring, addition of a damping force in the out-of-plane direction can make the system matrix better conditioned. However, this damping force may generate unnecessarily high resistance to the movement of the cloth.

[Baraff and Witkin 1998] used a linear elastic model for both stretching and compression. Although their formulation looks different from ours, we can make the similarity apparent by converting their formulation to that of the linear spring model. If we define the behavior function (as they refer to it) as $\mathbf{c} = |\mathbf{x}_{ij}| - L$, then the force vector will be same as Equation 2 and consequently the Jacobian $\partial \mathbf{f}/\partial \mathbf{x}$ will also be the same. Therefore, when the spring is compressed, the Jacobian matrix has negative eigenvalues in the orthogonal direction as indicated above. [Baraff and Witkin 1998] reduced the possibility of the system matrix becoming indefinite by the inclusion of a specially designed damping force. In their formulation, the damping force for stretch/compression does not contribute to the out-of-plane motion, but the damping force for bending acts along the out-of-plane direction. This damping force for bending will help to make the system matrix better conditioned at the cost of adding resistance to the out-of-plane movement of the cloth. Unfortunately there is still no guarantee that the damping will make the matrix positive definite.

In our formulation, a highly stiff linear spring is used only for tension. Therefore the system matrix is guaranteed to be positive definite, and no additional damping term is needed to cure the divergence problem. However, the cloth may shrink under compressive load if no compression resistance is included in the model. In our method, the *type 2* interaction model simultaneously accounts for compression and bending, and consequently the buckling problem is handled in a single interaction model.

## 3.2 Our Solution to the Post-Buckling Instability

As mentioned above, buckling causes serious stability problems in physical simulations of cloth. It is interesting to note that buckling has quite different meanings in rigid materials and textile fabrics. Buckling means a failure in rigid materials, whereas it means success in textile fabrics [Amirbayat and Hearle 1989]. The post-buckling behavior in rigid materials is quite destructive, while the same behavior in textile fabrics naturally evolves into the shapes that are the essence of a fabric's appearance. We refer to [Amirbayat and Hearle 1989] for this fabric-specific property. Although there are clear distinctions between the buckling behavior of fabrics and rigid materials, they are not reflected in most existing cloth simulation techniques. Since our solution to the post-buckling instability is based on the distinguished feature of fabric buckling, we clarify the concept of buckling in this section.

First, we analyze the buckling of a rigid material in terms of solid mechanics. We then contrast this phenomenon with the buckling of textile fabrics. Consider the idealized rigid column shown in Figure 3(a), which consists of two rigid bars connected at point $C$ by a rotational spring of stiffness $k_\theta$. In this configuration, the bending resistance is condensed at point $C$. Now, suppose an axially compressive force $P$ is applied at point $A$. Since the rotational spring resists bending, the two bars remain straight at equilibrium (Figure 3(b)). Now, suppose that the structure under force $P$ is disturbed by an external force that causes a small lateral movement of point $C$ (Figure 3(c)). The compressive force $P$ will try to increase the
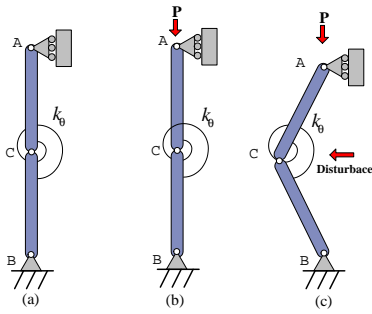
Figure 3: Column Buckling



(a) before buckling  (b) after buckling

Figure 4: Simplified Structure for Type 2 Interaction



(a) $P/k_b$=23.50  (b) $P/k_b$=35.25

Figure 5: Numerical Solutions of Moment Equilibrium Equation

lateral displacement, while the rotational spring will try to restore the system to the original straight position. Suppose that the disturbance is removed at this moment. If $P$ is relatively small, the bars will return to the straight position (i.e. the structure is stable). However, if $P$ is relatively large the lateral displacement will become larger and larger (i.e. the structure is unstable), and the structure will eventually collapse by lateral buckling. The magnitude of the axial force at which the structure bifurcates into either the stable or unstable condition by application of an infinitesimal increase or decrease in force is known as the critical load and is denoted by $P_{cr}$. At the critical load, the deflection of the structure is mathematically arbitrary. Once the axial load exceeds $P_{cr}$ the structure collapses and the original shape cannot be recovered, regardless of the degree to which the load exceeds $P_{cr}$, and no matter how quickly the load is reduced back to a value less than or equal to $P_{cr}$.

Now, let us consider the behavior when a fabric buckles. As for rigid materials, a textile fabric will buckle when subjected to an axial force greater than the critical load. When it buckles, it exhibits an unstable post-buckling response similar to that found in rigid materials. In contrast to rigid materials, however, fabrics do not break or collapse. Instead, they quickly pass the unstable state and reach a stable equilibrium (a smoothly bent shape). Moreover, the bent shape tends to return to the original straight shape when the axial load is removed [Amirbayat and Hearle 1989].

As described above, textile fabrics pass through an unstable state when they buckle. The simulation of this unstable post-buckling response requires special care if divergence problems are to be avoided. Once the material goes into the unstable post-buckling state, the deflection increases even when the load decreases. In other words, the stiffness of the material in the buckling direction is instantaneously negative. Especially in semi-implicit methods where the internal force is explicitly predicted with derivatives [Baraff and Witkin 1998; Volino and Magnenat-Thalmann 2000], this structural instability makes the system matrix extremely ill-conditioned or indefinite, and a large time step often leads to divergence. There have been a number of efforts to avoid this post-buckling instability in the analysis of cloth deformation. For example, [Eischen et al. 1996] used an adaptive arc-length control of the load-deflection curve, and [Yu et al. 2000] employed an explicit method with fictitious damping to avoid divergence.

We solve the structural instability problem by predicting the static post-buckling response. The approach developed here is based on the above observations regarding fabric-specific behavior. The concept underlying our approach is that since the fabric quickly passes the unstable post-buckling state to reach a stable equilibrium, it has little chance to get into the unstable post-buckling state at the discrete time steps of the simulation. Thus we assume that the fabric is not in the unstable post-buckling state at any time step. Then, in calculating the internal force at each time step, we can evaluate the deformation energy in the area where the cloth buckles
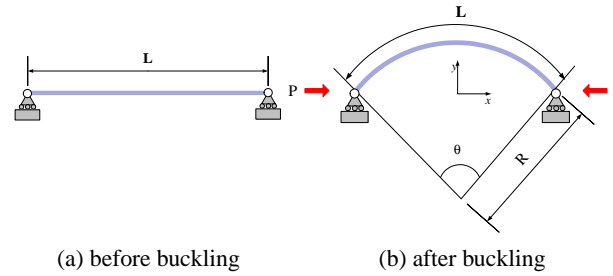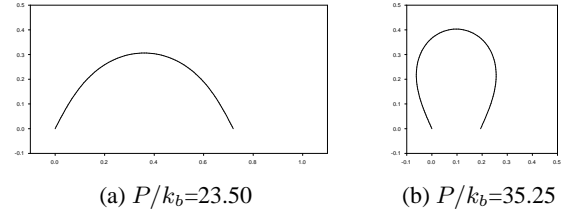
from the locally estimated deformed shape, which corresponds to the shape at the static equilibrium after buckling. The details of this procedure are presented in the next section. Unless the time step is miniscule, the loss of accuracy resulting from the approximated buckling response will be much less than the accuracy loss (and instabilities) resulting from the plain implicit time stepping. The approximated response model relieves the burden of *simulating* the unstable post-buckling dynamic response. According to our simulations, the approximated response model generates very realistic cloth motion with significantly improved stability. Wrinkle formation was quite natural. The simulation could be performed with a large step size.

### 3.3  Type 2 Interaction

The *type 2* interaction model is responsible for the post-buckling response created by compressive and bending forces. We predict the shape of the fabric after buckling and calculate the deformation energy from the deformed shape as described in the previous section.

The beam structure shown in Figure 4(a) approximates the region between two particles. Prior to buckling, the structure is a straight beam of length $L$.

After the structure buckles under a compressive load (Figure 4(b)), it will eventually reach a stable equilibrium structure. To predict the equilibrium shape, we use the moment equilibrium equation under the pinned ends condition[Gere 2001], which is given by

$$k_b\kappa + Py = 0, \tag{4}$$

where $k_b$ is the flexural rigidity, $\kappa$ is the curvature, $P$ is the compressive load, and $y$ is the deflection. Because we are modeling systems with large deflections, we cannot use the approximation $\kappa = y''$. Using the exact expression for the curvature[2], we obtained several numerical solutions corresponding to different values of $k_b$

---

[2]For a more general moment equilibrium equation for the analysis of fabric buckling, see [Kang et al. 2001].

and $P$. Two of these solutions are shown in Figure 5. The results show that the shape after buckling is close to a circular arc even when the deformation is large. Therefore, we approximated the equilibrium shape as a circular arc with constant arc length. As an alternative, we could have constructed a table of the numerical solutions of the moment equation at various values of $\frac{P}{k_b}$ for more accurate analysis. This was not undertaken because the results produced using the circular arc assumption were quite realistic. The bending deformation energy can be calculated from the estimated shape using the relation:

$$E = \frac{1}{2}\int_0^L \mathbf{M}\kappa dx \tag{5}$$

where $\mathbf{M}$ is the bending moment and $\kappa$ is the curvature. Taking into account the linear relationship between the curvature and bending moment, and the constant curvature through the structure, the integral yields the solution:

$$E = \frac{1}{2}k_b L \kappa^2, \tag{6}$$

where $k_b$ is the flexural rigidity. Since the arc length is assumed to be the same as the initial straight length $L$, the curvature $\kappa$ can be expressed solely in terms of the distance $|\mathbf{x}_{ij}|$ between the two extremities.

$$\kappa = \frac{2}{L}\mathrm{sinc}^{-1}(\frac{|\mathbf{x}_{ij}|}{L}), \tag{7}$$

where $\mathrm{sinc}(x) = \frac{\sin x}{x}$.

The force vector is derived as,

$$\mathbf{f}_i = k_b\kappa L \frac{d\kappa}{d|\mathbf{x}_{ij}|}\frac{\mathbf{x}_{ij}}{|\mathbf{x}_{ij}|} = k_b\kappa L \left(\frac{d|\mathbf{x}_{ij}|}{d\kappa}\right)^{-1}\frac{\mathbf{x}_{ij}}{|\mathbf{x}_{ij}|} \tag{8}$$

$$= k_b\kappa^2(\cos\frac{\kappa L}{2} - \mathrm{sinc}(\frac{\kappa L}{2}))^{-1}\frac{\mathbf{x}_{ij}}{|\mathbf{x}_{ij}|} \tag{9}$$

$$\equiv f_b(|\mathbf{x}_{ij}|)\frac{\mathbf{x}_{ij}}{|\mathbf{x}_{ij}|} \tag{10}$$

The blue curve in Figure 6 depicts the dependence of $f_b$ on the distance between particles (approximated with a fifth order polynomial function). The unit of each axis in this graph is made dimensionless. The system shows the following behavior. When the compression force $P$ is initially applied (top right corner of Figure 6), the structure remains straight until the load reaches the buckling load $P_{cr}$. However, in real systems geometric imperfections in the structure cause the fabric to start to buckle at the onset of loading, giving an actual curve (the green curve in the graph) that exhibits finite deflection even at small magnitudes of the compression force, and asymptotically approaches $f_b$ as compressive force increases [Gere 2001]. To model this characteristic, we used the function $f_b^*$ in our final implementation:

$$f_b^* = \begin{cases} c_b(|\mathbf{x}_{ij}| - L) & : & f_b < c_b(|\mathbf{x}_{ij}| - L) \\ f_b & : & \text{otherwise} \end{cases} \tag{11}$$

where $c_b$ is a constant of our choice, usually assigned a value comparable to $k_s$. Although we could have used a higher order function to model the deflection at small values of the compression force, we found no significant difference in the results obtained using higher order functions and those obtained with the linear function $c_b(|\mathbf{x}_{ij}| - L)$ (red curve in Figure 6).

The Jacobian matrix of the force vector is derived as

$$\frac{\partial \mathbf{f}_i}{\partial \mathbf{x}_j} = \frac{df_b^*}{d|\mathbf{x}_{ij}|}\frac{\mathbf{x}_{ij}\mathbf{x}_{ij}^T}{\mathbf{x}_{ij}^T\mathbf{x}_{ij}} + \frac{f_b^*}{|\mathbf{x}_{ij}|}(\mathbf{I} - \frac{\mathbf{x}_{ij}\mathbf{x}_{ij}^T}{\mathbf{x}_{ij}^T\mathbf{x}_{ij}}). \tag{12}$$
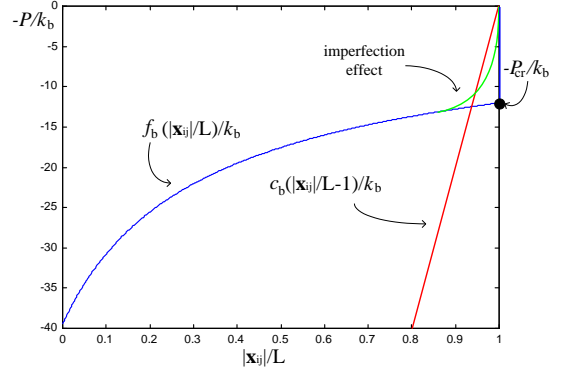


Figure 6: Nondimensionalized Curves of $P$ vs. $|\mathbf{x}_{ij}|$

In the above equation, $\frac{df_b^*}{d|\mathbf{x}_{ij}|}$ is always positive but $\frac{f_b^*}{|\mathbf{x}_{ij}|}$ is always negative, creating the possibility that the second term could turn the system matrix indefinite. To guarantee the positive definiteness of the system matrix, we dropped this term and thus the force in the orthogonal direction is not affected by implicit filtering. Although this force is not filtered, there is little possibility that the system will diverge even when a large time step is employed because the magnitude of this force is very small compared to the stretch force, and it is always finite. Note that in a model where the repulsive and contractive forces are equally strong, dropping the orthogonal term can make the system unstable under a large time step unless the bending resistance is of comparable strength.

The above discussion of the type 2 interaction model highlights the necessity of interlacing the type 2 connections in the manner shown in Figure 2(b). If only sequential connections were used, the global shape could be bent without increasing the bending energy provided that each local connection maintained the initial distance.

### 3.4 Damping

The physical model described above is quite stable; thus, there is no need for additional energy dissipative terms to stabilize the numerical procedure. However, we do need to consider the intrinsic damping property of fabrics. Without an appropriate (material intrinsic) damping term, the simulated fabric can exhibit large unrealistic in-plane oscillations. To include this type of damping, we added a simple linear damper along the direction of interaction.

The damping force exerted on particle $i$ from the interaction with particle $j$ is given by,

$$\mathbf{f}_i = -k_d(\mathbf{v}_i - \mathbf{v}_j) \tag{13}$$

and the Jacobian matrix is simply expressed as,

$$\frac{\partial \mathbf{f}_i}{\partial \mathbf{v}_j} = k_d\mathbf{I}. \tag{14}$$

Note that the force term in Equation 13 does not add any damping to the orthogonal direction. This is important because the most interesting fabric deformation occurs in the out-of-plane direction.

The above force term does not create a filtering effect under a semi-implicit formulation when the cloth undergoes a linear rigid motion (i.e., when the velocity vectors of all the particles are identical). This is the case because for such a motion the $3\times3$ block-wise row sums of the matrix $\frac{\partial \mathbf{f}}{\partial \mathbf{v}}$ are $3\times3$ zero matrices from the above equations, and the rigid motion vector $\mathbf{v}_{rigid}$ is an eigenvector of

$\frac{\partial \mathbf{f}}{\partial \mathbf{v}}$ with zero eigenvalue. Therefore, there is no implicit filtering effect caused by $\frac{\partial \mathbf{f}}{\partial \mathbf{v}}$. Even when the $\frac{\partial \mathbf{f}}{\partial \mathbf{x}}$ terms in Equations 3 and 12 are included in the system equation, there will be no implicit filtering to the rigid motion, provided that all the interacting directions of particle $i$ are orthogonal to $\mathbf{v}_i$ for all $i$ and that the cloth is not stretched, since the $\frac{\partial \bar{\mathbf{f}}}{\partial \mathbf{x}}$ terms in Equations 3 and 12 also produce null vectors when multiplied by $\mathbf{v}_{rigid}$. Therefore, the motion to the orthogonal direction would not be filtered under a semi-implicit formulation.

In more general situations, even though the above condition is not met, our formulation has very small artificial damping in the out-of-plane direction, which potentially makes the cloth movement look more realistic.

## 4   Numerical Integration

We use semi-implicit integration with a second-order backward difference formula (BDF). The $k$-th order BDF is defined as,

$$\frac{d}{dt} = \frac{1}{\Delta t} \sum_{q=1}^{k} \frac{1}{q} (\Delta^{-1})^q, \qquad (15)$$

where

$$\Delta^{-1}\mathbf{x} = \mathbf{x}^{n+1} - \mathbf{x}^n.$$

For $k = 2$, the discretization of $\dot{\mathbf{x}}$ becomes,

$$\dot{\mathbf{x}} = \frac{1}{\Delta t}(\frac{3}{2}\mathbf{x}^{n+1} - 2\mathbf{x}^n + \frac{1}{2}\mathbf{x}^{n-1}). \qquad (16)$$

Considering both performance and accuracy, we chose second order BDF for the semi-implicit formulation. The second order BDF creates less artificial damping than the first order BDF, but is equally stable.

The state equation of motion

$$\left( \begin{array}{c} \dot{\mathbf{x}} \\ \dot{\mathbf{v}} \end{array} \right) = \left( \begin{array}{c} \mathbf{v} \\ \mathbf{M}^{-1}\mathbf{f} \end{array} \right) \qquad (17)$$

is discretized with the second order BDF as

$$\frac{1}{\Delta t}\left( \begin{array}{c} \frac{3}{2}\mathbf{x}^{n+1} - 2\mathbf{x}^n + \frac{1}{2}\mathbf{x}^{n-1} \\ \frac{3}{2}\mathbf{v}^{n+1} - 2\mathbf{v}^n + \frac{1}{2}\mathbf{v}^{n-1} \end{array} \right) = \left( \begin{array}{c} \mathbf{v}^{n+1} \\ \mathbf{M}^{-1}\mathbf{f}^{n+1} \end{array} \right). \quad (18)$$

The nonlinear term $\mathbf{f}^{n+1}$ in the above equation is replaced with

$$\mathbf{f}^{n+1} = \mathbf{f}^n + \frac{\partial \mathbf{f}}{\partial \mathbf{x}}(\mathbf{x}^{n+1} - \mathbf{x}^n) + \frac{\partial \mathbf{f}}{\partial \mathbf{v}}(\mathbf{v}^{n+1} - \mathbf{v}^n). \qquad (19)$$

By combining Equations 18 and 19, we can obtain a linear system rearranged either for $\Delta^{-1}\mathbf{x}$ or $\Delta^{-1}\mathbf{v}$. If we rearrange the linear system for $\Delta^{-1}\mathbf{x}$, the equation becomes,

$$(\mathbf{I} - \Delta t \frac{2}{3}\mathbf{M}^{-1}\frac{\partial \mathbf{f}}{\partial \mathbf{v}} - \Delta t^2 \frac{4}{9}\mathbf{M}^{-1}\frac{\partial \mathbf{f}}{\partial \mathbf{x}})(\mathbf{x}^{n+1} - \mathbf{x}^n)$$
$$= \frac{1}{3}(\mathbf{x}^n - \mathbf{x}^{n-1}) + \frac{\Delta t}{9}(8\mathbf{v}^n - 2\mathbf{v}^{n-1})$$
$$+ \frac{4\Delta t^2}{9}\mathbf{M}^{-1}(\mathbf{f}^n - \frac{\partial \mathbf{f}}{\partial \mathbf{v}}\mathbf{v}^n) - \frac{2\Delta t}{9}\mathbf{M}^{-1}\frac{\partial \mathbf{f}}{\partial \mathbf{v}}(\mathbf{x}^n - \mathbf{x}^{n-1}). \quad (20)$$

The linear system of Equation 20 is sparse and generally unbanded. We solve this system using a preconditioned conjugate gradient method. We used a $3 \times 3$ block diagonal matrix for the preconditioner, which showed an improvement of approximately 20% over the diagonal preconditioner. In addition, we assessed other preconditioners such as IC and ILU but found no performance gain though the number of iterations decreased.

## 5   Collision Handling

Collision detection and response model is not a contribution of this paper. In this section, we briefly describe how we handled collisions in our implementation.

To detect collisions we use a voxel-based collision detection algorithm similar to that proposed by [Zhang and Yuen 2000]. After voxelizing the space in which the cloth is enclosed, we register each cloth particle and solid triangle to the corresponding voxels based on their spatial coordinates. Then, we independently perform collision detection for each voxel. This voxelization method locates the possible collisions very efficiently and shows nearly linear performance.

We detect the cloth-solid collision by checking the particle-triangle pairs to determine if particles are beneath the solid surface. To avoid missing pairs near the voxel boundaries, the triangles are redundantly registered to the nearby voxels. When a collision is detected, the particle's next displacement along the normal direction of the colliding surface is determined, and this constraint is enforced using the invariant method in the conjugate gradient iteration proposed in [Baraff and Witkin 1998]. For the tangential direction, we add a frictional force that is proportional both to the constraint force and to the velocity difference between the solid surface and the particle in contact.

To test for self-collision, we check the particle-particle pairs. If the particles are too close, we simply add a repulsive proximity force between the colliding particles. The Jacobian matrix of this force is made to have null eigenvalues in the directions orthogonal to the repelling direction as in the case of the *type 2* interaction model in Section 3.3.

## 6   Results

This section reports the results from several simulations. The animations of these simulations can be found at http://graphics.snu.ac.kr/∼kjchoi/cloth.htm

Table 1 summarizes the performance of our algorithm on a Pentium3-550 machine. In this table, the CPU sec/frame field cites the total CPU time required to carry out all of the steps (i.e., collision detection, linear system setup, conjugate gradient iteration, etc.) required to produce one frame of 30 Hz animation. For all the simulations, the collision detection time was less than 20% of the total CPU time. The mesh resolutions of the clothes in the animations were about $L = 1 \sim 2cm$.

For the simulations involving human motions (Animations 1∼4), the time step was fixed to $\Delta t = 1/90s$ throughout the animation; thus the simulator produced one frame of 30 Hz animation with three time steps. The simulations were stable despite the use of a fixed time step. All attempts to use a time step greater than 1/90s encountered collision handling failures before the stability limit was reached.

In Animation 1(a), the character is wearing a one-piece made of a thin fabric. The nature of the fabric was controlled by assigning a small value to the bending rigidity. The character walks at a normal pace without any fast movements. Nevertheless the cloth motion is quite responsive; the wrinkle details delicately form and disappear. However, we considered the cloth motion in Animation 1(a) to be more responsive than would be expected for a real cloth. To produce a more fabric-like motion, we increased the bending rigidity and intrinsic damping, and reduced the frictional force. The result was Animation 1(b). Animations 2 and 3 contain more vigorous character motions, which created very dynamic movement of the cloth and wrinkles. In Animation 4 the character is wearing jeans. The jeans fabric was modeled by assigning it a high bending rigidity and a high resistance to buckling. The animation produced the

Table 1: Performance Summary

| animation | | # particles of cloth | # triangles of solid | CPU sec/ frame | time step (s) |
|---|---|---|---|---|---|
| 1(a) | | 5608 | 13802 | 6.13 | 0.011 |
| 1(b) | | 5579 | 13802 | 5.86 | 0.011 |
| 2 | | 5579 | 15308 | 5.68 | 0.011 |
| 3 | top | 3396 | 15308 | 2.98 | 0.011 |
| | skirt | 3456 | 15308 | 3.01 | 0.011 |
| 4 | top | 3294 | 14324 | 3.25 | 0.011 |
| | pants | 6624 | 14324 | 7.01 | 0.011 |
| 5 | | 2601 | 0 | 0.18 | 0.2 |



| t=0.4s | t=1.4s | t=3.4s | t=10.0s |
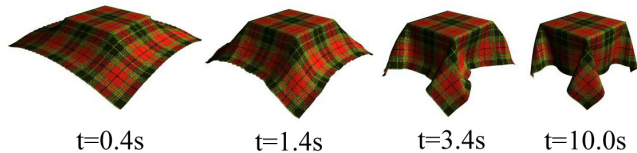
Figure 7: Snapshots from Animation 5 : Stability Test ($\Delta t = 0.2s$)

buckled shapes near the knees and ankles quite well, which are frequently observed in real jeans. Several snapshots taken from each of the animations 1∼4 are shown in Figure 8.

Animation 5 was designed purely to determine the maximum time step that could be used in our cloth animation technique; it was not intended as a realistic animation. The simulation modeled a square of fabric draped over a solid box, as shown in Figure 7. To exclude the collision detection problem we did not explicitly include the box; Instead, we simply constrained the movement of the sub-square region of the fabric. Additionally, we disabled both self-collision and solid-collision. Under the above conditions, we verified that the algorithm runs stably with time step sizes up to *100s*, although the resulting animation was very choppy and it required hundreds of time steps for the fabric to settle down to the final shape. Such a large time step is not meaningful and cannot possibly generate realistic animation because the derivatives have no significance after 100 seconds. A marginally acceptable animation with self-collision enabled was obtained with $\Delta t = 0.2s$. Several snapshots taken during this animation are shown in Figure 7.

Although there is no established method or system for validating the dynamic motion of cloth, our technique produced animations that are visually quite believable. It is noteworthy that these animations were obtained using a reasonable, practical amount of computation.

## 7 Conclusion

The groundbreaking work of [Baraff and Witkin 1998] on implicit time stepping greatly reduced the computational cost of integrating the stiff equations used in simulating textile fabrics, and thereby provided a practical solution for animating clothed characters. However, the phenomenon of buckling, which is another source of instability and a crucial property in cloth deformation, has been largely ignored until now. If the buckling problem cannot be handled appropriately, natural cloth animation would require enormous (almost impractical) amount of computation.

This paper represents the first report of a stable and practical method to handle the post-buckling instability without introducing a damping force into the dynamic simulation. The proposed method was shown to produce very realistic motion of clothes made from a range of fabric types using a uniform time step size. In particular, the power of the new method was shown in the animation of a light and thin cloth where sensitive response of cloth is required, which was very difficult to produce using the previous methods.

The tremendously increased stability of our algorithm allowed the simulation of the motion of cloth with time steps of 0.2 seconds or longer which could not be achieved in previous methods.

## References

AMIRBAYAT, J., AND HEARLE, J. 1989. The anatomy of buckling of textile fabrics : Drape and conformability. *Journal of Textile Institute 80*, 1, 51–70.

BARAFF, D., AND WITKIN, A. 1998. Large steps in cloth simulation. In *Proceedings of SIGGRAPH 98*, ACM Press / ACM SIGGRAPH, Computer Graphics Proceedings, Annual Conference Series, ACM, 43–54.

BATHE, K. J. 1996. *Finte Element Procedures*. Prentice-Hall.

BREEN, D. E., HOUSE, D. H., AND WOZNY, M. J. 1994. Predicting the drape of woven cloth using interacting particles. In *Proceedings of SIGGRAPH 94*, ACM Press / ACM SIGGRAPH, Computer Graphics Proceedings, Annual Conference Series, ACM, 365–372.

CARIGNAN, M., YANG, Y., MAGNENAT-THALMANN, N., AND THALMANN, D. 1992. Dressing animated synthetic actors with complex deformable clothes. In *Computer Graphics (Proceedings of ACM SIGGRAPH 92)*, ACM, 99–104.

COURSHESNES, M., VOLINO, P., AND MAGNENAT THALMANN, N. 1995. Versatile and efficient techniques for simulating cloth and other deformable objects. In *Proceedings of SIGGRAPH 95*, ACM Press / ACM SIGGRAPH, Computer Graphics Proceedings, Annual Conference Series, ACM, 137–144.

DESBRUN, M., SCHRÖDER, P., AND BARR, A. 1999. Interactive animation of structured deformable objects. In *Graphics Interface*, 1–8.

EBERHARDT, B., WEBER, A., AND STRASSER, W. 1996. A fast, flexible, particle-system model for cloth draping. *IEEE Computer Graphics and Applications 16*, 5 (Sept.), 52–59.

EISCHEN, J. W., DENG, S., AND CLAPP, T. G. 1996. Finite-element modeling and control of flexible fabric parts. *IEEE Computer Graphics and Applications 16*, 5 (Sept.), 71–80.

GERE, J. M. 2001. *Mechanics of Materials*. Brooks/Cole.

KANG, T., JOO, K., AND LEE, K. 2001. Analysis of fabric buckling based on nonlinear bending properties. *(Submitted)*, http://textile.snu.ac.kr/upjuk/PDF/IJ_TRJ_2002_KHJOO.PDF.

PROVOT, X. 1995. Deformation constraints in a mass-spring model to describe rigid cloth behavior. In *Graphics Interface '95*, 147–154.

TERZOPOULOS, D., AND FLEISCHER, K. 1988. Modeling inelastic deformation: Viscoelasticity, plasticity, fracture. In *Computer Graphics (Proceedings of ACM SIGGRAPH 88)*, ACM, 269–278.

VOLINO, P., AND MAGNENAT-THALMANN, N. 2000. Implementing fast cloth simulation with collision response. In *Proceedings of the Conference on Computer Graphics International (CGI-00)*, 257–268.

VOLINO, P., AND MAGNENAT-THALMANN, N. 2001. Comparing efficiency of integration methods for cloth animation. In *Proceedings of the Conference on Computer Graphics International (CGI-01)*.

YU, W., KANG, T., AND CHUNG, K. 2000. Drape simulation of woven fabrics by using explicit dynamic analysis. *Journal of Textile Institute 91 Part 1*, 2, 285–301.

ZHANG, D., AND YUEN, M. 2000. Collision detection for clothed human animation. In *Proceedings of the 8th Pacific Graphics Conference on Computer Graphics and Application (PACIFIC GRAPHICS-00)*, 328–337.

Figure 8: Snapshots from Animations 1∼4. Each animation corresponding to each row shows different materials with different parameters.